Cell Calcium 92 (2020) 102307

Contents lists available at ScienceDirect

Cell Calcium

journal homepage: www.elsevier.com/locate/ceca

Inhibition of TRPM7 with waixenicin A reduces glioblastoma cellular functions

Raymond Wong [a,b], Haifan Gong [a,b], Rahmah Alanazi [a,b], Andrew Bondoc [e], Amanda Luck [e], Nesrin Sabha [f], F. David Horgen [g], Andrea Fleig [h], James T. Rutka [a,*], Zhong-Ping Feng [b,*], Hong-Shuo Sun [a,b,c,d,*]

[a] Departments of Surgery, Faculty of Medicine, University of Toronto, Toronto, Canada
[b] Department of Physiology, Faculty of Medicine, University of Toronto, Toronto, Canada
[c] Department of Pharmacology, Faculty of Medicine, University of Toronto, Toronto, Canada
[d] Leslie Dan Faculty of Pharmacy, University of Toronto, Toronto, Canada
[e] Departments of Cell Biology SickKids Research Institute, The Hospital for Sick Children, Toronto, Canada
[f] Departments of Genetics and Genome Biology, SickKids Research Institute, The Hospital for Sick Children, Toronto, Canada
[g] Department of Natural Sciences, Hawaii Pacific University, Kaneohe, Hawaii, 96744, USA
[h] Center for Biomedical Research at The Queen's Medical Center and John A. Burns School of Medicine at the University of Hawaii, Honolulu, Hawaii, 96720, USA

ARTICLE INFO

Keywords:
TRPM7
waixenicin A
ion channels
glioblastoma
drug target

ABSTRACT

Glioblastoma (GBM) is the most common malignant primary brain tumour originating in the CNS. Median patient survival is <15 months with standard treatment which consists of surgery alongside radiation therapy and temozolomide chemotherapy. However, because of the aggressive nature of GBM, and the significant toxicity of these adjuvant therapies, long-term therapeutic effects are unsatisfactory. Thus, there is urgency to identify new drug targets for GBM. Recent evidence shows that the transient receptor potential melastatin 7 (TRPM7) cation channel is aberrantly upregulated in GBM and its inhibition leads to reduction of GBM cellular functions. This suggests that TRPM7 may be a potential drug target for GBM treatment. In this study, we assessed the effects of the specific TRPM7 antagonist waixenicin A on human GBM cell lines U87 or U251 both *in vitro* and *in vivo*. First, we demonstrated *in vitro* that application of waixenicin A reduced TRPM7 protein expression and inhibited the TRPM7-like currents in GBM cells. We also observed reduction of GBM cell viability, migration, and invasion. Using an intracranial xenograft GBM mouse model, we showed that with treatment of waixenicin A, there was increased cleaved caspase 3 activity, alongside reduction in Ki-67, cofilin, and Akt activity *in vivo*. Together, these data demonstrate higher GBM cell apoptosis, and lower proliferation, migration, invasion and survivability following treatment with waixenicin A.

1. Introduction

Glioblastoma (GBM) displays aggressive proliferative and diffuse invasive characteristics [1]. Patients diagnosed with GBM have poor survival rates and current treatment options have limited efficacy [2,3]. The first-line chemotherapeutic compound, temozolomide, is non-specific and a somewhat toxic alkylating agent. Therefore, in search of a more effective treatment, there is urgency to identify safer drug alternatives that can target and inhibit GBM with greater specificity.

Ion channels are a growing target class for drug development. In GBM, certain members from the transient receptor potential (TRP) superfamily of ion channels are upregulated [4–7]. Our lab has previously demonstrated that both mRNA and protein expression of the transient receptor potential melastatin 7 (TRPM7) are upregulated in GBM when compared to normal human astrocytes [4]. TRPM7 is ubiquitously expressed in mammalian tissue, serving primarily as a Ca^{2+} and Mg^{2+} conductor [8]. In addition to TRPM7, a previous study [27] showed in the tumours of 33 GBM patients that other TRP channels were also

Abbreviations: GBM, glioblastoma; TRPM7, transient receptor potential melastatin 7; CNS, central nervous system; MPO, multiparameter optimization; BBB, blood brain barrier; FBS, fetal bovine serum; HEK, human embryonic kidney.

* Corresponding authors at: Temerty Faculty of Medicine, University of Toronto, Toronto, Ontario, M5S 1A8, Canada.
E-mail addresses: james.rutka@sickkids.ca (J.T. Rutka), zp.feng@utoronto.ca (Z.-P. Feng), hss.sun@utoronto.ca (H.-S. Sun).

https://doi.org/10.1016/j.ceca.2020.102307
Received 3 August 2020; Received in revised form 27 September 2020; Accepted 4 October 2020
Available online 14 October 2020

upregulated, including TRPM3, TRPM8, TRPC1, TRPC6, TRPV1, and TRPV2. Thus, these other TRP channels may also contribute to Ca^{2+} homeostasis in GBM. The closely related TRPM6 which also conducts Mg^{2+} (like TRPM7) was also examined, but it was not found to be upregulated in GBM [27]. Based on the present literature, TRPM7 and the metal transporter CNNM3 are the primary candidates in GBM responsible for transporting Mg^{2+} and involved in Mg^{2+} homeostasis [52], although much remains to be elucidated.

Previous reports showed that the intracellular levels of free Mg^{2+} are elevated (twofold and above) in GBM tumours compared to the normal brain [54]. Moreover, aberrant Mg^{2+} upregulation has been suggested to play a role in contributing to enhancing GBM malignancy [54]. Based on this rationale, Mg supplements can potentially promote GBM cellular functions, including viability. Interestingly, it was shown in another cancer type (colon adenocarcinoma) that TRPM7 inhibition by waixenicin A induced hypomagnesemia which reduced cell proliferation in vitro, and Mg supplementation was unable to reverse this [23].

In addition to GBM, there is growing body of evidence suggesting that reducing TRPM7 activity inhibits various other cancer cells [9–14], thus suggesting potential broader implications. Previously, our lab reported that both 1) pharmacological inhibition of TRPM7 channels with the non-specific TRPM7 inhibitors carvacrol or xyloketal B; and 2) silencing of TRPM7 via siRNA-mediated knockdown in GBM reduced cellular functions *in vitro* such as proliferation, migration and invasion [4,5]. We also provided additional evidence for the involvement of TRPM7 in GBM cellular functions with an alternative approach, showing that potentiation of TRPM7 activity with the selective agonist naltriben enhanced GBM migration and invasion [15]. However, in order to further evaluate the potential of TRPM7 as a drug target for GBM treatment, it is necessary to assess the effects of a pharmacological inhibitor that is specific to TRPM7 particularly in *in vivo* evaluations. Little has been written on the topic of the use of specific TRPM7 inhibitors and cancer. Therefore, our study will help fill the knowledge gap in this area.

In HEK293 cells overexpressing TRPM7, waixenicin A has been reported to inhibit channel activity with an IC_{50} of 16 nM [16] which makes it the most potent antagonist known in the literature. The specificity of waixenicin A for TRPM7 has also been closely examined; it was demonstrated that even 10 μM waixenicin A failed to inhibit the closely homologous TRPM6, and also did not affect TRPM4, TRPM2, or CRAC (Ca^{2+} release-activated Ca^{2+}) channels in HEK293 cell lines overexpressed with the respective channel [16]. Because TRPM6 is most structurally similar to TRPM7, the lack of effect of waixenicin A on this ion channel provided strong evidence for its specificity.

Therefore, in the present study, we evaluated the TRPM7-specific antagonist waixenicin A using a combination of *in vitro* and *in vivo* approaches. First, we investigated *in vitro* the effects of waixenicin A on the cellular functions of GBM cell lines U251 or U87 using the following assays to assess cellular functions: MTT (viability), Oris migration and wound healing scratch (migration), and Matrigel Transwell (invasion). Additionally, we used Western immunoblots and patch-clamp electrophysiology to determine the effects of waixenicin A on TRPM7 protein expression and functional/channel activity, respectively. Furthermore, we explored the potential underlying mechanisms of waixenicin A effects *in vivo* by employing an intracranial xenograft GBM mouse model. Here, we provide the first report in GBM showing the effects of waixenicin A on animal survival and drug tolerance, as well as demonstrating the potential signalling cascades downstream of TRPM7 underlying the observed functional outcomes. We show that that TRPM7 inhibition by the specific inhibitor waixenicin A can inhibit the neoplastic phenotype of GBM.

2. Materials and Methods

2.1. Waixenicin A

This natural marine compound isolated from the Hawaiian soft coral *Sarcothelia edmondsoni* is a potent and specific inhibitor of the TRPM7 ion channel [16]. Waixenicin A has been extensively tested in various TRPM channel overexpressed HEK293 cells [16] as well as in primary neurons [17] for its specificity of TRPM7 inhibition. Furthermore, a central nervous system multiparameter optimization (CNS MPO) analysis [18] calculates that waixenicin A has a high index for blood brain barrier (BBB) permeability property, with the brain/plasma equilibration rate of −3.1, which delineates "brain penetration sufficient for CNS activity". Isolated compound was stored in single use aliquots in a desiccated oxygen-free environment, and reconstituted in methanol just prior to use.

2.2. Cell culture

U251 and U87 human GBM cell lines were obtained from the American Type Culture Collection (Manassas, VA). Cells were grown at 37 °C (5% CO_2; 95% humidified air) on culture dishes (10 cm) in Dulbecco's modified Eagle's medium (DMEM) supplemented with fetal bovine serum (FBS; 10%), and 100 U/mL penicillin and streptomycin. Cell culture materials, including fetal bovine serum (FBS) and Dulbecco's modified Eagle's medium (DMEM) were purchased from Gibco Life Technologies Corporation (USA).

2.3. Electrophysiology

An Axopatch 700B (Axon Instruments, Inc) was used for patch-clamp recordings (whole-cell configuration) of U251 or U87 cells to examine waixenicin A's effects on TRPM7-like currents, with the following protocol: voltage ramp from –100 to +100 mV over 400 ms, 5 s interval, and at 2 kHz (5 kHz digitized). Note that we have previously assessed waixenicin A in TRPM7-overexpressed HEK293 cells and confirmed TRPM7 current inhibition [22]. pClamp 9.2 and Clampfit 9.2 were used for data acquisition and analyses, respectively. Recordings were conducted at room temperature. When filled with intracellular solution, pipette resistance was 5–10 MΩ. The intracellular pipette solution contained 145 mM CsMSF, 10 mM HEPES, 8 mM NaCl, 0.5 mM $MgCl_2$, and 10 mM EGTA (pH 7.2, adjusted with CsOH). The extracellular bath solution contained 20 mM HEPES, 140 mM NaCl, 2 mM $CaCl_2$, 5 mM KCl, 10 mM glucose (pH 7.4, adjusted with NaOH; osmolarity ~300 mOsm, adjusted with sucrose).

2.4. Cell viability and proliferation assay

U251 or U87 cells (5×10^4 cells/mL) were cultured on 96-well plates. Cells were treated for 24 h with either vehicle control (3% methanol) or waixenicin A at varying concentrations (125, 250, 500, or 1000 nM). Afterwards, MTT reagent (5 mg/mL; 1:10 dilution) was added into each well, and incubated (3 h, 37 °C, 5% CO_2). Mitochondrial enzymes reduced yellow MTT into purple formazan (insoluble). Medium was then discarded, and the formazan was dissolved in DMSO (100 μL). Viability of cells was quantified using a microplate reader (Syngery H1, Biotek, USA) by measuring the amount of formazan at 490 nm absorbance, and was expressed as a percentage of vehicle control. Four independent experiments were performed, where each repeat consisted of four samples per group (i.e. vehicle control, and waixenicin A at each concentration).

2.5. Wound healing assay

5×10^4 cells/mL U87 or U251 cells were grown to >90% confluency on surface-treated culture plates. A 200 μL pipette tip was used to scratch the monolayer of cells, creating a wound gap. After washing, cells were administered vehicle (3% methanol; control) or 500 nM waixenicin A treatment. A phase-contrast microscope (Olympus CKX41, Japan; ×10 objective) was used to image the same visual field of cells throughout the experiment. To minimize the effects of proliferation

during the experimental period, cells were maintained in low FBS (1%) medium. Wound closure was quantified in ImageJ with the following formula: percentage of closure = Gap(T-T_0)/GapT_0×100% (where T = duration of treatment; T_0 = scratch induction).

2.6. Oris cell migration assay

The Oris migration assay was performed following the manufacturer's instructions (Platypus Technologies, USA). In brief, U251 cells were seeded into the provided Oris 96-well plate at 2.5 × 10^4 cells/mL and kept in a humidified incubator at 37 °C with 5% CO_2 for 18 hours to allow attachment. The stopper in each well was removed to create a circular exclusion zone in the cell layer that was then washed once with sterile PBS to discard detached cells. Culture medium containing 1% FBS and control (3% methanol in PBS) or 500 nM waixenicin A was added to each well. The plate was incubated at 37 °C with 5% CO_2 to allow migration. An Olympus microscope (4× objective) was used to capture a phase contrast micrograph of each well 0, 12, 24, and 48 hours post-treatment. The area of the wound in each image was analyzed using ImageJ and percentage of closure (%) was calculated using the formula: percentage of closure = Gap(T_{24}-T_0)/GapT_0 ×100% (where T_{24} = 24 h after treatment; T_0 = scratch induction).

2.7. Matrigel invasion assay

Cell invasion of U251 or U87 was assessed according to the Corning Matrigel Transwell chambers (8-μm polycarbonate Nucleopore filters, BD Biosciences) manufacturer's instructions. In brief, cells were treated with vehicle (3% methanol; control) or 500 nM waixenicin A for 24 h, and then 100 μL of FBS-free DMEM containing 2.5 × 10^4 cells/mL cells were placed in the top chamber. In the bottom chamber, 600 μL of complete medium served as a chemoattractant. Actively invading cells would cause degradation of the Matrigel, thus migrating to the top chamber's lower membrane surface. Methanol (100%) was used to fix invaded cells, which were then stained with 1% Toluidine blue. Images of invading cells were taken via a CKX41 Olympus microscope, and then quantified using ImageJ.

2.8. Western immunoblot

U251 cells were seeded into 60 mm culture dishes and grown to >50% confluency. Cell culture medium containing either control (3% methanol in PBS) or 500 nM waixenicin A was added to each dish, which was then incubated in a humidified incubator at 37 °C with 5% CO_2 for 24 h. The cell layer was then scraped and re-suspended in ice-cold RIPA buffer, which contained: 20 mM Tris-HCl (pH 7.5), 150 mM NaCl, 1% NP-40, 0.5% sodium deoxycholate, 0.1% SDS, protease inhibitors (1 μg/mL pepstatin A, 5 μg/mL leupeptin, 2 μg/mL aprotinin, 1 mM sodium orthovanadate, 0.1 mM PMSF, and 10 mM NaF). Protein concentration was measured with Pierce BCA Protein Assay Kit (Thermo Fisher scientific, USA). Samples were then heat-treated at 95 °C for 5 min, and 40 μg from each was separated on a gradient SDS-PAGE gel (6% + 10%). Samples were transferred to a 0.2 μm PVDF membrane (Bio-Rad, USA) at 120 V for 90 min on ice and blocked with 5% skim milk in TBS-T on a rocking platform for 1 h at room temperature. The membranes were then incubated in primary antibodies overnight at 4 °C: anti-TRPM7 (1:1000, ab85016, Abcam, USA) or anti-GAPDH (1:5000, 2118S, CST, USA). Next, membranes were incubated in respective mouse (1:7500, 7076S, CST, USA) or rabbit (1:10000, 7074S, CST, USA) secondary antibodies in 5% skim milk. Protein signals were detected using film (Clonex, CA) after incubation with enhanced chemiluminescence reagent (Bio-Rad, USA). The intensity of each protein band was analyzed using ImageJ.

2.9. Orthotopic GBM xenotransplantation and drug treatment

All animal experiments were conducted according to the policies and regulations of the Institutional Animal Care and Use Committee (IACUC) at The Centre for Phenogenomics (Toronto, ON, Canada) as previously described [19,20,21]. In brief, female NOD *scid* gamma mice (~8 weeks of age, n = 5/group) were administered analgesic subcutaneously (meloxicam 2 mg/kg). Consistent with previous studies [19,20], females were preferred over males due to a more consistent brain size and morphology over time (i.e. males continue to get larger with age, whereas females remain approximately the same size after approximately eight weeks). Animals were placed under anaesthesia using 4% isoflurane in 100% oxygen. The depth of anaesthesia was assessed by pedal withdrawal reflex. Mice were placed in prone position on a warmed stereotaxic frame (Stoelting Co, Wood Dale, IL, USA), where their heads were immobilized in a horizontal position via ear bars. A 5 mm sagittal incision was made over the parietal skull, and a micro-drill (Blackstone Industries, Bethel, CT, USA) was used to create a hole in the skull at the following coordinates: from bregma suture, medial-lateral 1 mm right, anterior-posterior 0 mm. Intracranial injection of 5 × 10^4 U251 cells in 2.5 μL PBS into the caudoputamen was performed using a 32 gauge syringe (Hamilton Company, Reno, NV, USA) at a depth of 3.5 mm ventral to the skull surface. Note that the U251 cell line was chosen for intracranial injections because we found that, in our hands, it induced formation of tumours quicker and more uniform *in vivo* compared to the U87 cell line. After withdrawing the needle, the hole and incision were closed using bone wax and interrupted vicryl sutures, respectively. Mice were administered fluids and closely monitored for general health as they recovered. At three weeks following tumour induction, 20 μL/g of vehicle or waixenicin A (at a dose of 8 μg/g; concentration adapted from a previous publication where waixenicin A was safely used in an adenocarcinoma *in vivo* model [23]) was delivered once daily, in a blinded manner, via intraperitoneal (i.p.) injections for a period of 14 days. Treatment continued until signs of tumour burden were evident, at which point mice were euthanized by CO_2 inhalation. Animal brains were extracted, sectioned coronally, fixed in 10% formalin for 48 h, and embedded in paraffin blocks. Brain slices were stained with hematoxylin and eosin (H&E) to determine histopathological features.

2.10. Immunohistochemistry

Prior to immunostaining, 5 μm thick paraffin sections were deparaffinized, rehydrated, and pretreated in citrate buffer (pH 6.0) for 15 min. Sections were blocked in 10% goat serum and incubated (1 h, room temperature) in one of the following primary antibodies: Ki-67 (1:100, Biocare Medical), p-Akt (1:100, Origene), p-cofilin (1:100, Sigma), and cleaved caspase-3 (1:100, Cell Signaling). After three washes, biotinylated secondary antibody 1:100 (ABC kit, Vector Labs) was applied for 30 min at room temperature, and then incubated (40 min, room temperature) in the Avidin-Biotin detection system. After three washes, signal was detected using DAB, counterstained with hematoxylin, and mounted using Permount (Thermo Fisher Scientific). Whole slides images were captured with an Aperio AT2 (Leica Biosystems) and micrographs were captured with an Infinity1 camera (Lumenera Corporation) with eponymous software visualized through an Olympus BX43 light microscope (Olympus). For each brain, three coronal layers were analyzed to obtain a greater comprehensive representation of the tumour. As previously described in the literature [19,21], two methods of quantification were conducted: 1) a colorimetric algorithm in Aperio ImageScope software was used to quantify the percentage of positive DAB brown signal representing Ki67, p-Akt, p-cofilin, or cleaved caspase 3 over a designated area of tissue (relative mask area, rMA); 2) number of cells (unstained or DAB brown stained) was counted in five to ten separate images representing all the tumour regions for each coronal layer. The percentage of stained cells was calculated and averaged

across all images. Imaging and quantification were done in a blinded manner.

2.11. Statistical analysis

All data are presented as the mean with the standard error of mean, where $p < 0.05$ was considered to be statistically significant. For comparison between two groups, Student's *t*-tests were used, whereas one-way ANOVA (with subsequent Bonferroni test) was used for multiple comparisons. The Kaplan-Meier estimate with log-rank test was used to generate survival curves. Statistical analysis was conducted with GraphPad Prism 6 (GraphPad Software, San Diego, USA)

3. Results

3.1. U251 and U87 cell viability reduced by waixenicin A in a dose dependent manner

First, we assessed U251 and U87 cell viability with or without waixenicin A treatment via the MTT assay. As shown in Fig. 1A, treatment with waixenicin A for 24 h significantly reduced viability of both U251 and U87 cells in a dose dependent manner when compared to vehicle control (3% methanol; $p < 0.01$; n=16/group). The degree of cell viability inhibition by waixenicin A (~25%) is consistent with findings from our previous studies where we suppressed TRPM7 with other drugs or knockdown with siRNA [4,5]. For both cell lines, we observed that potency of waixenicin A on GBM cell viability had a plateau starting at 500 nM (i.e. no further effects with greater concentration). One explanation for this concentration plateau may be due to the binding affinity of waixenicin A to TRPM7 in GBM, which has been shown to be mediated by intracellular magnesium [16]. Thus, we used waixenicin A at 500 nM when assessing other parameters of GBM cellular functions *in vitro*. Interestingly, 500 nM waixenicin A was also the optimal concentration to confer neuroprotective effects following hypoxic stress *in vitro*, as reported in our previous hypoxic-ischemic brain injury study [22].

3.2. Waixenicin A reduced TRPM7 protein expression and inhibited endogenous TRPM7-like current in GBM

Next, we examined whether waixenicin A treatment affects TRPM7 protein expression in GBM. After treating U251 cells with either vehicle or 500 nM waixenicin A for 24 h, we measured the TRPM7 expression with Western immunoblots. As shown in Fig. 1B, waixenicin A reduced TRPM7 protein level (1.54 ± 0.21 versus 0.99 ± 0.17 TRPM7/GADPH ratio for vehicle and waixenicin A groups, respectively; $p < 0.05$; n=4/group).

We then asked whether acute application of waixenicin A can inhibit TRPM7 activity in GBM. Recently, we showed that 500 nM waixenicin A inhibited TRPM7 current in the tetracycline-inducible stably-transfected TRPM7 HEK293 cells [22]. In the present study, we assessed whether waixenicin A can inhibit the endogenous TRPM7-like currents in U251 and U87 cells via patch-clamp electrophysiology using the whole cell configuration. As shown in Fig. 1C, there was spontaneous TRPM7-like current showing the characteristic large outwardly rectification in both U251 and U87 cells, consistent with our previous studies [4,5]. Following perfusion of waixenicin A (500 nM; 5 min), the TRPM7-like current at +80 mV was significantly reduced from 9.26 ± 1.47 pA/pF to 3.08 ± 1.19 pA/pF in U251 cells ($p < 0.01$; n=5/group), and from 8.21±1.74 pA/pF to 3.94±0.74 pA/pF in U87 cells ($p < 0.001$; n=4/group). Our observations show that the endogenous TRPM7-like current in U251 or U87 cells can be inhibited by acute application of waixenicin A. We applied waixenicin A acutely (5 min) in order to show in the same cell the TRPM7 current before and after drug perfusion. Thus, each cell served as its own control. Additionally, the acute timeframe also gave stronger evidence that the reduction in TRPM7 activity was due to inhibition of the channel. At 24 hours, because we also observed downregulation of the TRPM7 protein, patch clamp evaluation at this point would be less conclusive whether waixenicin A can directly modulate channel activity.

These results suggest that, in GBM, waixenicin A can: 1) reduce the protein expression of TRPM7; and 2) inhibit its current (Fig. 1B and 1C, respectively).

3.3. GBM migration and invasion were reduced with waixenicin A application in vitro

Migration of U251 or U87 was first evaluated with the classical wound healing scratch assay. As shown in Fig. 2, images of migrating cells with or without 500 nM waixenicin A treatment were taken at 0, 6, 12, 18 and 24 hours. Analysis of the wound gap revealed that: for U251 control, gap closure was 43.89 ± 4.03%, 74.40 ± 1.71%, 79.57 ± 1.46%, and 98.87 ± 0.28% at 6, 12, 18 and 24 hours, respectively (n = 6); whereas waixenicin A-treated U251 migration was significantly reduced with gap closure at 18.45 ± 2.57%, 51.37 ± 1.98%, 54.46 ± 2.31%, and 82.03 ± 3.12%, for the respective time points (n = 6; $p < 0.01$). A similar trend was observed for U87 migration: for control, gap closure was 22.87±2.09%, 43.04±2.84%, 84.77±2.93%, and 95.58±1.51% (n=6) at 6, 12, 18 and 24 hours, respectively; and significantly reduced with waixenicin A treatment, with gap closure at 8.09±0.72%, 27.67±3.65%, 53.38±7.31%, and 81.84±3.33%, respectively (n=6, $p < 0.05$).

To further examine GBM cell migration, we employed the Oris cell migration assay, which uses cell seeding stoppers to create highly consistent exclusion zones to monitor closure due to migrating cells [20]. As shown in Fig. 3A, we also observed reduction in migration when U251 cells were treated with 500 nM waixenicin A (n = 6) when compared with vehicle control (n = 7). Analysis of exclusion zone closure showed significant reduction at 24 h (control, 14.57 ± 1.87%; waixenicin A, 8.45 ± 0.68%; $p < 0.05$) and 48 h (control, 25.36±4.63%; waixenicin A, 10.94±3.20%; $p < 0.05$).

U251 or U87 invasion was then assessed with the Matrigel Transwell assay. As shown in Fig. 3B, application of waixenicin A (500 nM; 24 h) significantly reduced U251 or U87 invasion. For U251, relative invasiveness decreased from 99.99 ± 6.57% to 71.65 ± 2.33% with treatment of waixenicin A ($p < 0.01$; n=6/group). Similarly, waixenicin A also decreased U87 invasion from 100.00±4.46% to 69.11±3.48% ($p < 0.001$; n=6/group).

In summary, these findings showed that waixenicin A can reduce the migration and invasion of GBM cell lines U251 or U87 *in vitro*. Note that all cells were maintained in low FBS conditions (1% or less) during the experimental period, which we have observed prevented observable cell proliferation in the timeframes of interest (i.e. two days or less).

3.4. Waixenicin A decreased Akt, Ki-67 and cofilin activity, and increased caspase 3 activity in GBM xenografts

Finally, we assessed the effects of waixenicin A *in vivo* using an intracranial xenograft GBM mouse model. Fig. 4A shows the timeline of the athymic NOD *scid* gamma mice used in this study. In brief, U251 cells were injected when mice were eight weeks old, and the tumour was allowed to grow for three weeks before onset of treatment. Animals were administered 20 μL/g of either vehicle or waixenicin A (8 μg/g) once/day; volumes were equal for both groups. Note that this concentration of waixenicin A was adapted from a previous publication where the drug was safely used in an adenocarcinoma mouse model [23]. Treatment was continued until the animals reached endpoint. As shown in Fig. 4B, although there was a trend towards slightly longer survival with waixenicin A treatment, Kaplan Meier analysis reported non-significance (p = 0.74; n = 5/group). This suggests that waixenicin A treatment alone is insufficient to prolong survival of animals with GBM. Waixenicin A was well tolerated by mice; Fig. 4C illustrates a slight trend towards reduced weight loss for waixenicin A-treated animals (21.28 ± 0.48% versus

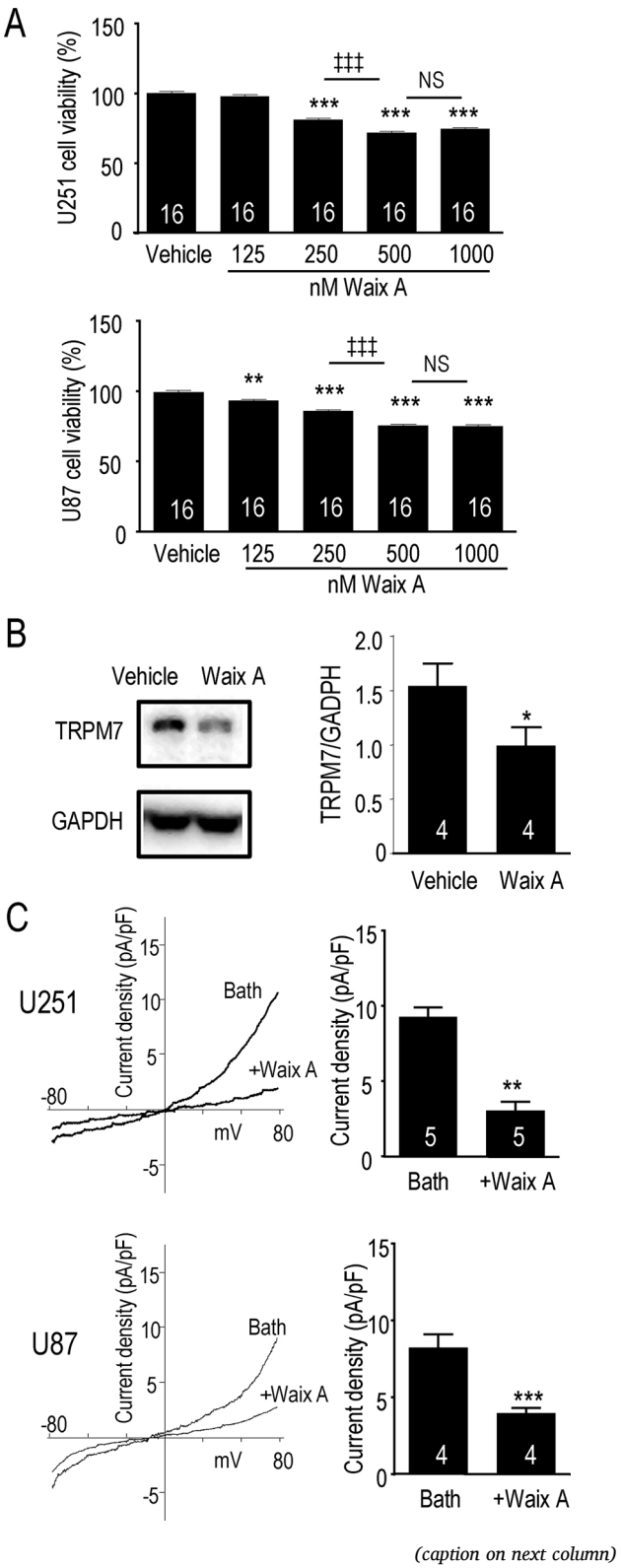

(caption on next column)

Fig. 1. Viability of U251 or U87 was reduced with waixenicin A-treatment, which also reduced TRPM7 protein expression and TRPM7-like current in GBM. A) Summary chart of MTT assay assessing U251 or U87 cell viability when treated for 24 h with vehicle control (3% methanol), or waixenicin A at 125, 250, 500 or 1000 nM (**, *** represent comparison with control, $p < 0.01$ and $p < 0.001$, respectively; ‡‡‡ represents comparison between 250 versus 500 nM waixenicin A, $p < 0.001$; One-way ANOVA, n=16/group). B) Representative image of Western immunoblot (left) and summary chart (right) comparing ratio of TRPM7 to GADPH in U251 cells that were treated with either vehicle control or 500 nM waixenicin A for 24 h (* represents $p < 0.05$; Student's *t*-test, n = 4/group). C) For U251 or U87 cells, [Left] representative traces showing spontaneous TRPM7-like current following break-in in bath solution. Perfusion with 500 nM waixenicin A for 5 min significantly reduced the current. [Top right] Summary chart for U251 comparing before and after waixenicin A perfusion (** represents $p < 0.01$; Student *t*-test, n = 5/group). [Bottom right] Summary chart for U87 comparing before and after waixenicin A perfusion (*** represents $p < 0.001$; Student *t*-test, n = 4/group).

19.58 ± 1.09% in vehicle and waixenicin A groups, respectively; $p = 0.19$; n=5/group).

Nonetheless, previous *in vitro* studies from our laboratory and others [4–7,24–26] demonstrated that inhibition of TRPM7 in cell culture reduced various signalling activities that contribute to GBM cellular functions, including: Ki-67 (proliferation), Akt (growth, invasion, survivability), cofilin (migration, invasion), and caspase 3 (apoptosis). In the present study, we examined whether treating GBM xenotransplanted mice with waixenicin A had any effects on the expression of the above markers in the tumour.

As shown in Fig. 5A (top two panels), H&E images illustrated that the histological features defining tumour presence, including hypercellularity, necrosis, and invasion, were present in the U251 GBM xenograft of all animals (both vehicle and waixenicin A groups). Measurement of tumour area from H&E images showed a trend of ~10% smaller tumour area in the waixenicin A group compared to vehicle (not statistically significant; data not shown); however, the limitations of interpreting two-dimensional tumour representations need to be considered. In the future, live imaging of the brain to obtain a three-dimensional representation of tumour would give a more accurate estimate of waixenicin A's effects on tumour mass and volume.

Following immunohistochemistry (images shown in Fig. 5A; bottom four panels), quantification of biomarker expression was done via both cell counting (CC) as well as algorithm detection (AD). Two analytical approaches were employed to get a more accurate overall representation of biomarker expression. Note that both techniques have been used in previous studies [19,21]. We compared vehicle versus waixenicin A groups (n = 5/group), respectively; in animals treated with waixenicin A, we observed a reduction in the activity of Ki-67 (CC: 52.65 ± 1.18% versus 43.94 ± 0.44%, $p < 0.001$; AD: 55.99±0.57% versus 42.84±0.56%, $p < 0.001$; Fig. 5B), p-Akt (CC: 42.26 ± 6.03% versus 18.98 ± 7.78%, $p = 0.045$; AD: 51.63±3.74% versus 20.78±7.79%, $p < 0.01$; Fig. 5C), and p-cofilin (CC: 38.03 ± 9.65% versus 66.98 ± 5.08%, $p = 0.029$; AD: 40.91±10.05% versus 69.04±3.51%, $p = 0.030$; Fig. 5D; note that phosphorylation leads to inactivity). We also observed an increase in caspase 3 activity (CC: 1.31 ± 0.42% versus 2.73 ± 0.39%, $p = 0.037$; AD: 1.49±0.48% versus 3.18±0.23%, $p = 0.014$; Fig. 5E). This suggested that waixenicin A-mediated effects on GBM *in vivo* may involve caspase 3, Ki-67, cofilin, and Akt signalling.

4. Discussion

Our study employed a combination of *in vitro* and *in vivo* approaches to show that application of waixenicin A in the GBM cell lines U251 and U87: 1) decreases TRPM7 protein expression; 2) inhibits endogenous TRPM7-like current; 3) reduce cell viability, migration and invasion; and 4) downregulates activity of Ki-67, Akt and cofilin, while upregulating caspase 3 activity. The evidence here suggests that the specific

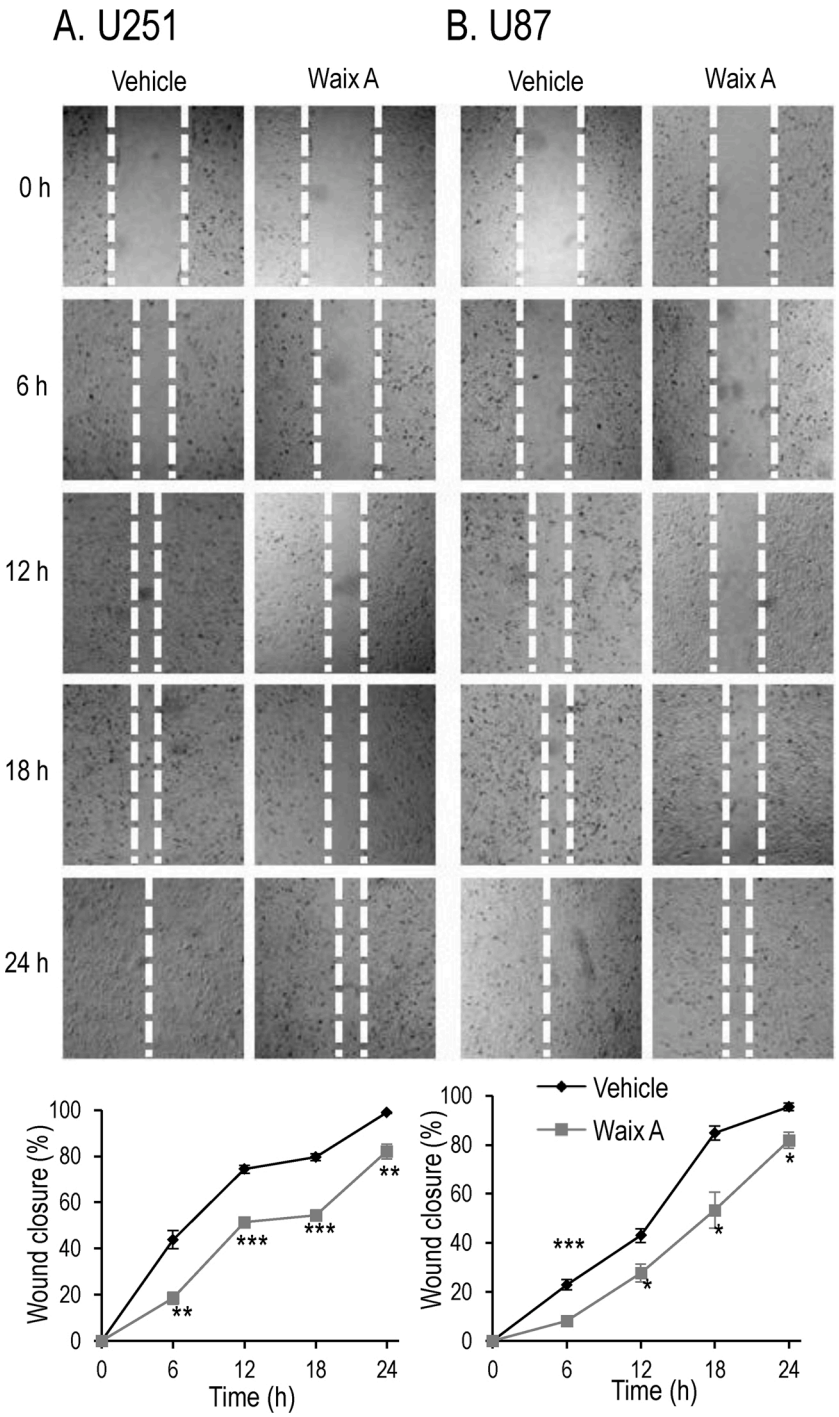

Fig. 2. Treatment with waixenicin A reduced gap closure after scratch induction of U251 or U87 cells. A) [Top] Representative images of U251 cells scratch wound healing after administering 3% methanol vehicle (control) or 500 nM waixenicin A. Images were captured at 0, 6, 12, 18, and 24 h. [Bottom] Summary chart showing that the gap closure of the waixenicin A-treated U251 cells was significantly reduced at 6–24 h compared to control cells at their respective time points (**,*** represent $p < 0.01$, $p < 0.001$, respectively; Student *t*-test, n = 6/group). B) [Top] Representative images of U87 cells scratch wound healing after administering 3% methanol vehicle (control) or 500 nM waixenicin A. Images were then captured at 0, 6, 12, 18, and 24 h. [Bottom] Summary chart showing that the gap closure of the waixenicin A-treated U87 cells was significantly reduced at 6–24 h compared to control cells at their respective time points (*,*** represent $p < 0.05$, $p < 0.001$, respectively; Student *t*-test, n = 6/group).

TRPM7 inhibitor waixenicin A can potentially inhibit GBM growth and functions.

One important point to note is that the sensitivity of waixenicin A to TRPM7 is positively correlated to intracellular Mg^{2+} [16]. In the current study, waixenicin A was applied to cells where the internal Mg^{2+} was at the GBM cells' physiological levels. If internal Mg^{2+} were lowered, then waixenicin A would be less sensitive to TRPM7, and vice-versa for higher internal Mg^{2+}. Due to its Mg^{2+} dependence, the inhibitory mechanism of waixenicin A is unique compared to other known pharmacological inhibitors of TRPM7, which are nonspecific pore blockers and act independent of intracellular Mg^{2+} concentration. Examination of the TRPM7 channel kinase domain and its Mg^{2+} binding domain via mutagenesis showed interaction between Mg^{2+} and waixenicin A. Furthermore, it had been suggested that waixenicin A synergizes with internal Mg^{2+} to inhibit TRPM7 [16]. This unique mechanism of inhibition which may play a role in the drug's nanomolar potencies that is unprecedented in the other TRPM7 pharmacological inhibitors.

There is evidence that waixenicin A not only acts acutely on TRPM7 channel activity, but also reduces endogenous TRPM7 protein expression, as observed in the current study, as well as in a recent kidney fibrosis model [43]. While we currently do not know whether waixenicin A would be able to suppress heterologous TRPM7 expression also, expanding on this important observation is clearly warranted. Indeed, the modulation of TRPM7 protein expression as one of the drug's mode of action would likely enhance the therapeutic value of waixenicin A.

When compared to normal brain tissue, TRPM7 expression (mRNA

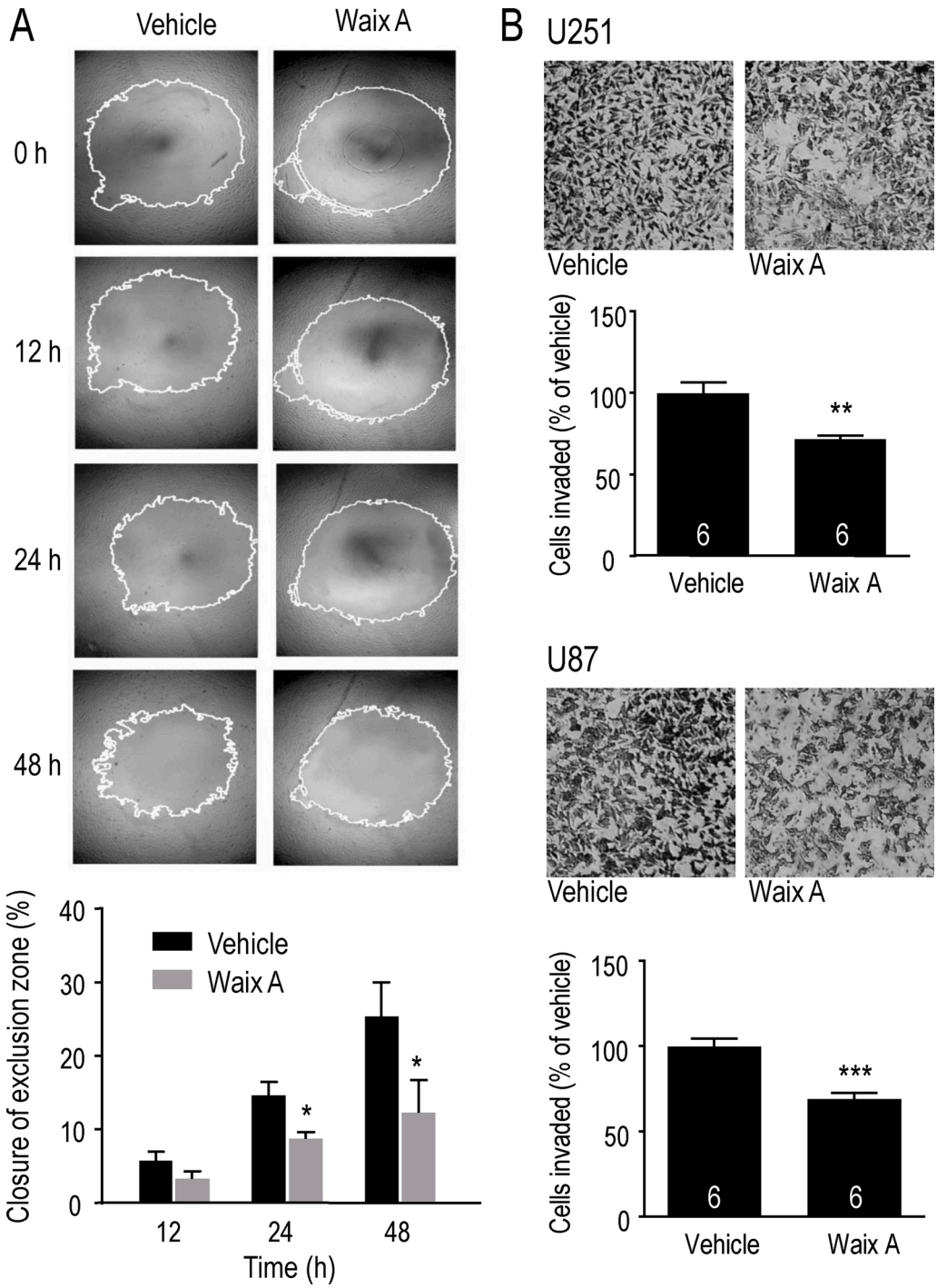

Fig. 3. Waixenicin A reduced radial migration and Matrigel invasion of GBM. A) [Top] Representative images of U251 migration with the Oris cell migration assay platform after treatment with vehicle (3% methanol) or waixenicin A (500 nM). Images were taken at 0, 12, 24, and 48 h. [Bottom] Summary chart showing that closure of exclusion zone was reduced significantly with waixenicin A at 24 and 48 h (* represents $p < 0.05$; Student *t*-test, n = 7/vehicle group, n = 6/waixenicin A group). B) [Top] Representative images of the Matrigel Transwell assay and summary chart assessing U251 cell invasion *in vitro*. Cells were treated with vehicle or 500 nM waixenicin A for 24 h. Invasion of U251 cells treated with waixenicin A was reduced at 24 h compared to control (** represents $p < 0.01$; Student *t*-test, n = 6/group). [Bottom] Representative images of the Matrigel Transwell assay assessing U87 cell invasion *in vitro*. Cells were treated with vehicle or 500 nM waixenicin A for 24 h. Invasion of U87 cells treated with waixenicin A was reduced at 24 h compared to control (*** represents $p < 0.001$; Student *t*-test, n = 6/group).

or protein) was aberrantly upregulated in GBM cell lines as well as primary tumours [4,27]. Additionally, transient knockdown of TRPM7 using virally mediated shRNA *in vivo* was shown to have no adverse effects in normal healthy rats [28]. However, a more recent study showed that under physiological conditions, conditional knockout of TRPM7 in mice impaired learning and memory [29]. Consequently, one key advantage to using a pharmacological approach is that TRPM7 inhibition is transient and can be mediated in order to minimize potential cognitive deficits. Waixenicin A treatment improved behaviour outcomes in mice that suffered from hypoxic-ischemic brain injury, and had no observed cognitive effects on sham animals [22]. Thus, pharmacologically inhibiting TRPM7 represents one potential therapeutic approach that can be specific to GBM with low toxicity to surrounding tissue.

Previously, our lab showed that the TRPM7-like currents in the GBM cell lines U251 or U87 can be pharmacologically inhibited with carvacrol or xyloketal B [4,5]. However, these compounds inhibit TRPM7 non-selectively and require higher concentrations to elicit effects (i.e. > 200 μM range *in vitro*), thus making non-specific TRPM7 antagonists less optimal to evaluate using *in vivo* models [4,5]. More recently, waixenicin A has been identified as a specific potent TRPM7 antagonist that has no effect on the closely related TRPM6 [16,17,30,31]. Here, we evaluated the effects of waixenicin A on GBM. This is important because there is an urgency to identify new compounds that are safer, and that have greater pharmacological specificity [1,3].

In the present study, we observed that acute application of

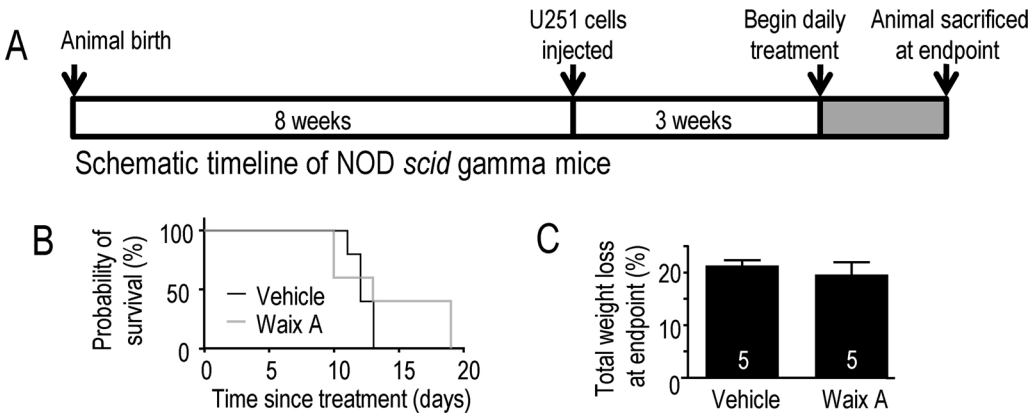

Fig. 4. Assessing waixenicin A *in vivo* using an orthotopic GBM brain tumour mouse model. A) Timeline showing stereotactic implantation of U251 cells in the right frontal lobe of eight-week old NOD *scid* gamma mice, followed by a three-week tumour growth period before the onset of daily treatment (grey zone). A volume of 20 μL/g of either vehicle or 8 μg/g waixenicin A was administered once/day until animals displayed signs of endpoint, at which point they were sacrificed. B) Kaplan-Meier survival curve illustrating the probability of animal survival (NS; $p > 0.05$) since the start of treatment with either vehicle (black line) or waixenicin A (grey line). C) Summary chart showing percentage of total animal weight loss between vehicle versus waixenicin A-treated mice (NS; $p > 0.05$; n=5/group).

waixenicin A robustly inhibited the TRPM7-like current in two GBM cell lines, consistent with previous findings using less-specific antagonists [4–7]. Waixenicin A has been tested extensively in various TRPM HEK293 overexpression systems in addition to primary cells by different labs [16,17,22,23]. Due to the specificity of waixenicin A for TRPM7, our results provided stronger evidence for channel identity. Furthermore, incubation of GBM with waixenicin A showed a reduction in TRPM7 protein expression. This suggests that, in addition to inhibiting TRPM7 current, waixenicin A can also reduce TRPM7 activity by downregulating its protein expression. This reduction in TRPM7 expression may be due to various mechanisms, including changes in gene transcription and translation, as well as protein trafficking and degradation [32]. Pharmacological TRPM7 inhibition with waixenicin A *in vitro* also reduced GBM proliferation, migration and invasion. These observations aligned with our past *in vitro* studies where we inhibited TRPM7 with other, less selective compounds [4,5]. This provides further evidence for our previous findings that reduction of GBM cellular functions was indeed through TRPM7-mediated effects.

There is growing evidence in the literature for the role of aberrant Ca^{2+} flux in contributing to GBM cellular functions [50]. One possible explanation for how TRPM7 inhibition reduces GBM cellular functions can be by impairing Ca^{2+} signalling. In addition to conducting Ca^{2+} directly, TRPM7 activity also modulates store-operated Ca^{2+} entry (SOCE). Specifically, it was shown that knockout of TRPM7 impaired SOCE by reducing the Ca^{2+}-release activated Ca^{2+} current [51]. Therefore, inhibition of TRPM7 via waixenicin A can potentially also reduce SOCE, which would impair Ca^{2+} signalling thus resulting in broad cellular implications.

We continued evaluation of waixenicin A in an *in vivo* GBM orthotopic brain tumour mouse model. Using a central nervous system multiparameter optimization (CNS MPO) [18], the structure of waixenicin A is predicted to have has sufficient brain penetration for CNS activity. Additionally, our lab previously demonstrated that waixenicin A conferred neuroprotective effects in an *in vivo* hypoxic-ischemic brain injury mouse model, wherein neuronal regeneration was promoted after insult [22]. These findings suggest that waixenicin A can cross the blood brain barrier *in vivo*. In addition, TRPM7 inhibition has been shown to protect against demyelination [33]. Considering that standard GBM treatments can adversely affect neurons [3], the broader implication is that waixenicin A has potential for dual benefit - that is, to reduce GBM cellular functions, while also providing neuroprotection from possible adverse effects caused by standard treatment. Moreover, our data provided evidence that waixenicin A was well tolerated by mice, which suggested drug safety.

The PI3K/Akt signalling pathway is aberrantly active in various cancers and plays key roles in a multitude of cellular functions, including proliferation, viability, migration and invasion [34–38]. However, since PI3K/Akt signalling is important for normal cell functions, drugs targeting this pathway may have non-specific/systemic effects outside the context of GBM, which can limit therapeutic benefit. Indeed, clinical trials evaluating pharmacological PI3K/Akt pathway inhibitors reported unsatisfactory patient response [39]. Consequently, a more effective strategy would involve targeting an upstream regulator of the PI3K/Akt pathway that has greater selectivity for GBM, such as TRPM7. There is growing evidence for the link between TRPM7 and PI3K/Akt. In GBM, previous reports from our lab showed that TRPM7 inhibition *in vitro* reduced p-Akt levels, and consequently downregulated its signalling [4,5]. TRPM7 also mediates the PI3K/Akt pathway in various other cell types. For example, levels of p-Akt were reduced after TRPM7 was silenced in human lung fibroblast and ovarian cancer cells [9,40]. In hepatic stellate cells, p-Akt expression generally increased with induction by platelet-derived growth factor, but this was prevented with TRPM7 knockdown [41]. In the current study, we provide the first report that *in vivo* waixenicin A treatment reduced p-Akt expression (suggesting downregulation of PI3K/Akt signalling) in an orthotopic GBM xenograft model, which is currently the most accurate model to predict drug effects in patients [42]. In addition, we also observed *in vivo* changes in several potential downstream effectors of Akt signalling; specifically, a downregulation in Ki-67 and cofilin activity, and an upregulation in caspase activity.

Firstly, Ki-67 is a key proliferation and viability marker used to determine the growth dynamics of GBM cell populations, and has been shown to be mediated in part through PI3K/Akt signalling [24]. The downregulation of Ki-67 expression with waixenicin A treatment observed here aligned with results from our *in vitro* viability and proliferation experiments. Consistent with this finding, another recent study showed that Ki-67 was also reduced following TRPM7 inhibition in unilateral ureter obstruction (UUO) kidneys [43].

Cofilin, an actin binding protein that is inactivated by phosphorylation, plays important roles for cell motility [44]. We recently provided evidence suggesting that cofilin signalling is downstream of TRPM7, as waixenicin A-treatment reduced cofilin activity in mice induced with hypoxic-ischemic brain injury [22]. Our previous *in vitro* study showed that inhibiting TRPM7 can subsequently reduce cofilin activity in GBM cells [4]. Additionally, evidence from our group demonstrated that knockdown or pharmacological inhibition of cofilin reduced glioma cell migration and invasion [26,45]. In patients, the cofilin pathway is highly upregulated in GBM compared to normal brain [26].

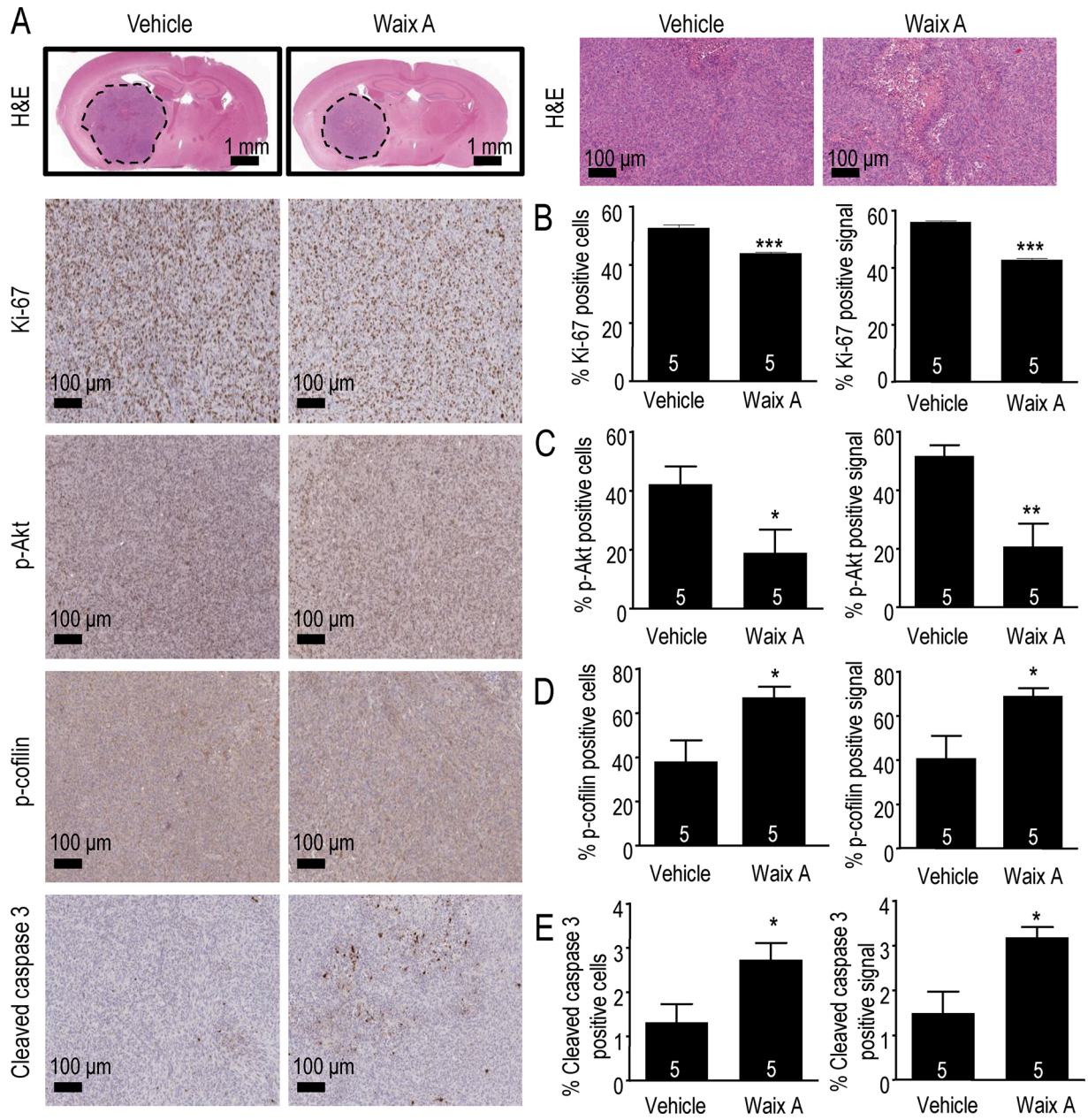

Fig. 5. Administering waixenicin A *in vivo* decreased Ki-67, Akt and cofilin activity, while caspase 3 activity was increased in GBM xenograft. A) [Top] Representative hematoxylin and eosin (H&E) images showing the presence of histological features defining tumour presence, such as hypercellularity, necrosis, and invasion. [Bottom] Representative immunohistochemistry images illustrating that, when compared with vehicle control, intracranial U251 tumours of animals that were treated once/day with 8 μg/g waixenicin A resulted in: B) decreased cell proliferation (Ki-76 staining; *** represents $p < 0.001$ for both cell counting [left panel] and algorithm detection [right panel] quantification methods; Student *t*-test, n = 5/group); C) decreased Akt signalling (p-Akt staining; *,** respectively represent $p < 0.05$ for cell counting [left panel], $p < 0.01$ for algorithm detection [right panel]; Student *t*-test, n = 5/group); D) decreased cell motility (p-cofilin staining; * represents $p < 0.05$ for both cell counting [left panel] and algorithm detection [right panel]; Student *t*-test, n = 5/group); and E) increased apoptosis (cleaved caspase 3 staining; * represents $p < 0.05$ for both cell counting [left panel] and algorithm detection [right panel]; Student *t*-test, n = 5/group).

Furthermore, tumour invasion has been linked with the cofilin activation status [45], thus targeting cofilin is an exciting direction of investigation that may represent a potential therapeutic target to reduce the GBM invasive machinery. In our *in vivo* evaluations, the reduction of cofilin activity in waixenicin A-treated animals aligned with results from our *in vitro* migration and invasion assessments. Interestingly, a recent report indicated the involvement of the SSH1/cofilin pathway in GBM [46], which can be regulated by PI3K/Akt signalling [47]. Accordingly, future GBM studies should explore whether TRPM7 has the potential to mediate cofilin activity through PI3K/Akt and SSH1 signalling.

Finally, caspase 3 in its active cleaved form signals the cell apoptotic cascade, and there is evidence suggesting its activity in GBM to be mediated in part by TRPM7 [4]. Caspase-mediated apoptosis is normally inhibited by Akt [25]. It is possible that the reduction in PI3K/Akt signalling with waixenicin A treatment observed here resulted in enhanced caspase activity, ultimately leading to lower GBM cell viability. Nevertheless, evidence detailing the molecular mechanisms underlying TRPM7 interaction with the PI3K/Akt pathway remains elusive in the literature. Since phospholipase C is involved in PI3K/Akt signalling, we speculate that the α-type Ser/Thr protein kinase domain of TRPM7 may interact with associated PLC isozymes [48]. This can subsequently interact with downstream receptor tyrosine kinases (RTK). Indeed,

recent evidence shows that TRPM7 inhibition reduced RTK activity in non-small cell lung cancer cells, which ultimately inhibited proliferation and migration [49]. Elucidating whether this mechanism also occurs in GBM is an important future direction in understanding the TRPM7-mediated effects (Fig. 6).

To summarize, TRPM7 inhibition with waixenicin A reduced GBM cellular functions *in vitro* and *in vivo*, potentially through reduction in PI3K/Akt activity and subsequent downstream signalling (Fig. 6). Nonetheless, further pre-clinical testing of waixenicin A's therapeutic potential is needed. Importantly, given that the *in vitro* reductions on GBM cellular functions by waixenicin A were modest, this may be one potential explanation for only observing a slight trend in improving animal survival *in vivo* via Kaplan Meier analysis. Thus, one key consideration for future evaluations include assessing waixenicin A in more animals. Additionally, previous reports by our group showed that there was breakdown of waixenicin A over 24 hours in serum [23]. Because fetal bovine serum was present in all cellular function assays, this represented one limiting factor of using waixenicin A that may explain its modest *in vitro* effects. When conducting these assays for future direction, one approach is to replenish waixenicin A at shorter intervals (i.e. 6 h) in GBM cells. In addition, future patch clamp investigations can examine whether the degradation products of waixenicin A also inhibit TRPM7 channel activity in GBM cells. To potentially address this chemical limitation of waixenicin A, our group is currently developing a synthesized version of the drug that has greater stability. Evaluating whether this improvement can potentially result in more robust effects on inhibiting GBM cellular functions *in vitro* and *in vivo* is a direction that we are pursuing for future studies. In order to gain a better understanding of TRPM7's role in human glioma, the next step is to assess waixenicin A in patient derived xenograft models. Other potential avenues of investigation include using a more stable synthesized version of the drug (a direction in which our group is currently working towards), dosage, mode of delivery, and/or frequency of administration. In conclusion, our current study provides further evidence in establishing TRPM7 as a potential drug development target for GBM treatment.

Funding

This work was supported by the following grants: NIH NIGMS P20 (GM103466) to FDH, Canadian Institutes of Health Research (CIHR 153104) to JTR and (CIHR PJT-153155) to ZPF, Natural Sciences and Engineering Research Council of Canada (NSERC) Discovery Grant (RGPIN-2016-04574) to HSS; NSERC Postgraduate Scholarship-Doctoral to RW.

Author Contributions

RW, HG, AL performed experiments; AB and NS assisted substantially to the in-vivo experiment; RW, HSS and ZPF wrote the manuscript; all authors discussed the results, analyzed data and commented on the manuscript; HSS and ZPF designed and developed the study.

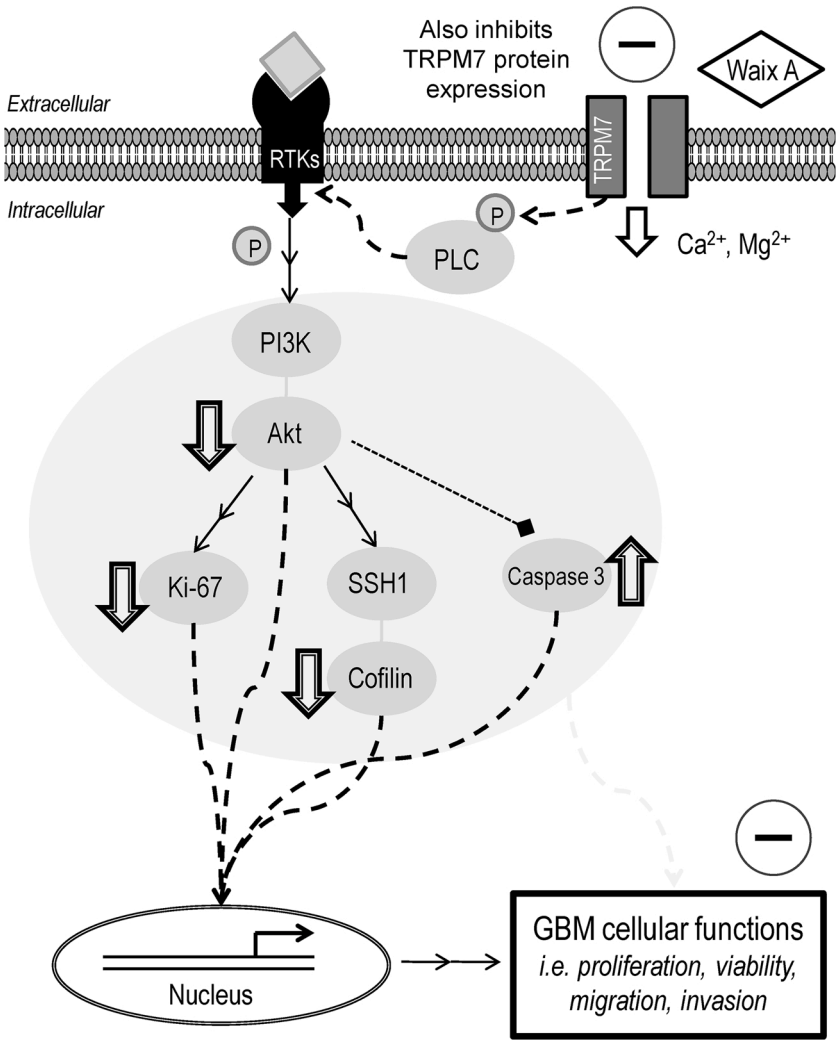

Fig. 6. Schematic detailing the intracellular signalling downstream of TRPM7, illustrating the potential underlying effects of waixenicin A-mediated TRPM7 inhibition. This schema details our current understanding of the potential signalling mechanism, based on the present work in conjunction with our previous studies. TRPM7 responds to intra- or extracellular stimuli via regulation of cation influx. Additionally, an α-type Ser/Thr protein kinase domain is present in TRPM7 that can phosphorylate surrounding cytosolic substrates like PLC. In turn, these can regulate the PI3K/Akt signalling and related downstream effectors including Ki-67, cofilin, and caspase 3. Consequently, GBM functional outcomes can be modulated via changes in gene transcription and translation, or via alternative cytosolic signalling. TRPM7 inhibition by waixenicin A downregulates activity of Ki-76, Akt and cofilin, and upregulates caspase 3 activity. Ultimately, this can potentially lead to reduction of GBM proliferation, viability, migration and invasion.

Declaration of Competing Interest

Authors declare no competing interests.

Acknowledgements

We thank WL Chen for his technical assistance.

References

[1] R. Stupp, W.P. Mason, M.J. van den Bent, M. Weller, B. Fisher, M.J. Taphoorn, K. Belanger, A.A. Brandes, C. Marosi, U. Bogdahn, J. Curschmann, R.C. Janzer, S. K. Ludwin, T. Gorlia, A. Allgeier, D. Lacombe, J.G. Cairncross, E. Eisenhauer, R. O. Mirimanoff, Radiotherapy plus concomitant and adjuvant temozolomide for glioblastoma, N. Engl. J. Med. 352 (2005) 987–996.

[2] J. Chen, J.S. Yakisich, Emerging concepts and therapeutic strategies for the treatment of brain tumors, Anticancer Agents Med. Chem. 14 (2014) 1063–1064.

[3] R. Stupp, M.E. Hegi, W.P. Mason, M.J. Van Den Bent, M.J. Taphoorn, R.C. Janzer, S.K. Ludwin, A. Allgeier, B. Fisher, K. Belanger, P. Hau, A.A. Brandes, J. Gijtenbeek, C. Marosi, C.J. Vecht, K. Mokhtari, P. Wesseling, S. Villa, E. Eisenhauer, T. Gorlia, M. Weller, D. Lacombe, J.G. Cairncross, R.O. Mirimanoff, Effects of radiotherapy with concomitant and adjuvant temozolomide versus radiotherapy alone on survival in glioblastoma in a randomized phase III study: 5-year analysis of the EORTC-NCIC trial, Lancet Oncol. 10 (2009) 459–466.

[4] W. Chen, A. Barszczyk, E. Turlova, M. Deurloo, B. Liu, B.B. Yang, J.T. Rutka, Z. P. Feng, H.S. Sun, Inhibition of TRPM7 by carvacrol suppresses glioblastoma cell proliferation, migration and invasion, Oncotarget 6 (2015) 16321–16340.

[5] W. Chen, E. Turlova, C.L.F. Sun, J.S. Kim, S. Huang, X. Zhong, Y.Y. Guan, G. L. Wang, J.T. Rutka, Z.P. Feng, H.S. Sun, Xyloketal B suppresses glioblastoma cell proliferation and migration in vitro through inhibiting TRPM7- regulated PI3K/Akt and MEK/ERK signaling pathways, Marine Drugs 13 (2015) 2505–2525.

[6] T.D. Leng, M.H. Li, J.F. Shen, M.L. Liu, X.B. Li, H.W. Sun, D. Branigan, Z. Zeng, H. F. Si, J. Li, J. Chen, Z.G. Xiong, Suppression of TRPM7 inhibits proliferation, migration, and invasion of malignant human glioma cells, CNS Neurosci, Ther. 21 (2015) 252–261.

[7] J. Liu, Y. Liu, Y. Ren, L. Kang, L. Zhang, Transmembrane protein with unknown function 16A overexpression promotes glioma formation through the nuclear factor-κB signaling pathway, Mol. Med. Rep. 9 (2014) 1068–1074.

[8] A. Fleig, R. Penner, The TRPM ion channel subfamily: Molecular, biophysical and functional features, Trends Pharmacol. Sci. 25 (2004) 633–639.

[9] J. Wang, L. Xiao, C.H. Luo, H. Zhou, J. Hu, Y.X. Tang, K.N. Fang, Y. Zhang, Overexpression of TRPM7 is associated with poor prognosis in human ovarian carcinoma, Asian Pac, J. Cancer Prev. 15 (2014) 3955–3958.

[10] Y. Sun, S. Selvaraj, A. Varma, S. Derry, A.E. Sahmoun, B.B. Singh, Increase in serum Ca^{2+}/Mg^{2+} ratio promotes proliferation of prostate cancer cells by activating TRPM7 channels, J. Biol. Chem. 288 (2013) 255–263.

[11] P. Rybarczyk, M. Gautier, F. Hague, I. Dhennin-Duthille, D. Chatelain, J. Kerr-Conte, F. Pattou, J.M. Regimbeau, H. Sevestre, H. Ouadid-Ahidouch, Transient receptor potential melastatin related 7 channel is overexpressed in human pancreatic ductal adenocarcinomas and regulates human pancreatic cancer cell migration, Int. J. Cancer 131 (2012) E851–E861.

[12] B.J. Kim, S.Y. Nah, J.H. Jeon, I. So, S.J. Kim, Transient receptor potential melastatin 7 channels are involved in ginsenoside Rg3-induced apoptosis in gastric cancer cells, Basic Clin. Pharmacol. Toxicol. 109 (2011) 233–239.

[13] J.P. Chen, Y. Luan, C.X. You, X.H. Chen, R.C. Luo, R. Li, TRPM7 regulates the migration of human nasopharyngeal carcinoma cell by mediating Ca^{2+} influx, Cell Calcium 47 (2010) 425–432.

[14] T. Hanano, Y. Hara, J. Shi, H. Morita, C. Umebayashi, E. Mori, H. Sumimoto, Y. Ito, Y. Mori, R. Inoue, Involvement of TRPM7 in cell growth as a spontaneously activated Ca^{2+} entry pathway in human retinoblastoma cells, J. Pharmacol. Sci. 95 (2004) 403–419.

[15] R. Wong, E. Turlova, Z.P. Feng, J.T. Rutka, H.S. Sun, Activation of TRPM7 by naltriben enhances migration and invasion of glioblastoma cells, Oncotarget 8 (2017) 11239–11248.

[16] S. Zierler, G. Yao, Z. Zhang, W.C. Kuo, P. Porzgen, R. Penner, F.D. Horgen, A. Fleig, Waixenicin A inhibits cell proliferation through magnesium-dependent block of transient receptor potential melastatin 7 (TRPM7) channels, J. Biol. Chem. 286 (2011) 39328–39335.

[17] E. Turlova, C.Y. Bae, M. Deurloo, W. Chen, A. Barszczyk, F.D. Horgen, A. Fleig, Z. P. Feng, H.S. Sun, TRPM7 regulates axonal outgrowth and maturation of primary hippocampal neurons, Mol. Neurobiol. 53 (2016) 595–610.

[18] T.T. Wager, X. Hou, P.R. Verhoest, A. Villalobos, Moving beyond rules: The development of a central nervous system multiparameter optimization (CNS MPO) approach to enable alignment of druglike properties, ACS Chem. Neurosci. 1 (2010) 435–449.

[19] D. Coluccia, C.A. Figueiredo, M.Y. Wu, A.N. Riemenschneider, R. Diaz, A. Luck, C. Smith, S. Das, C. Ackerley, M. O'Reilly, K. Hynynen, J.T. Rutka, Enhancing glioblastoma treatment using cisplatin-gold-nanoparticle conjugates and targeted delivery with magnetic resonance-guided focused ultrasound, Nanomedicine 14 (2018) 1137–1148.

[20] H. Okura, B.J. Golbourn, U. Shahzad, S. Agnihotri, N. Sabha, J.R. Krieger, C. A. Figueiredo, A. Chalil, N. Landon-Brace, A. Riemenschneider, H. Arai, C.A. Smith, S. Xu, S. Kaluz, A.I. Marcus, E.C. Van Meir, J.T. Rutka, A role for activated Cdc42 in glioblastoma multiforme invasion, Oncotarget 7 (2016) 56958–56975.

[21] C.C. Faria, B.J. Golbourn, A.M. Dubuc, M. Remke, R.J. Diaz, S. Agnihotri, A. Luck, N. Sabha, S. Olsen, X. Wu, L. Garzia, V. Ramaswamy, S.C. Mack, X. Wang, M. Leadley, D. Reynaud, L. Ermini, M. Post, P.A. Northcott, S.M. Pfister, S.E. Croul, M. Kool, A. Korshunov, C.A. Smith, M.D. Taylor, J.T. Rutka, Foretinib is effective therapy for metastatic sonic hedgehog medulloblastoma, Cancer Res. 75 (2015) 134–146.

[22] E. Turlova, R. Wong, B. Xu, F. Li, L. Du, S. Habbous, F.D. Horgen, A. Fleig, Z. P. Feng, H.S. Sun, TRPM7 mediates neuronal cell death upstream of calcium/calmodulin-dependent protein kinase II and calcineurin mechanism in neonatal hypoxic-ischemic brain injury, Transl. Stroke. Res. (2020), https://doi.org/10.1007/s12975-020-00810-3. Online ahead of print.

[23] J. Huang, H. Furuya, M. Faouzi, Z. Zhang, M. Monteilh-Zoller, F.K.G. Kawabata, F. D. Horgen, T. Kawamori, R. Penner, A. Fleig, Inhibition of TRPM7 suppresses cell proliferation of colon adenocarcinoma in vitro and induces hypomagnesemia in vivo without affecting azoxymethane-induced early colon cancer in mice, J. Cell, Commun. Signal. 15 (2017) 30.

[24] L. Miao, Z. Jiang, J. Wang, N. Yang, Q. Qi, W. Zhou, Z. Feng, W. Li, Q. Zhang, B. Huang, A. Chen, D. Zhang, P. Zhao, X. Li, Epithelial membrane protein 1 promotes glioblastoma progression through the PI3K/AKT/mTOR signaling pathway, Oncol. Rep. 42 (2019) 605–614.

[25] S.A. Valdes-Rives, D. Casique-Aguirre, L. German-Castelan, M.A. Velasco-Velazquez, A. Gonzalez-Arenas, Apoptotic signaling pathways in glioblastoma and therapeutic implications, Biomed. Res. Int. (2017), 7403747.

[26] J.B. Park, S. Agnihotri, B. Golbourn, K.C. Bertrand, A. Luck, N. Sabha, C.A. Smith, S. Byron, G. Zadeh, S. Croul, M. Berens, J.T. Rutka, Transcriptional profiling of GBM invasion genes identifies effective inhibitors of the LIM kinase-Cofilin pathway, Oncotarget 5 (2014) 9382–9395.

[27] M. Alptekin, S. Eroglu, E. Tutar, S. Sencan, M.A. Geyik, M. Ulasli, A.T. Demiryurek, C. Camci, Gene expressions of TRP channels in glioblastoma multiforme and relation with survival, Tumour Biol. 36 (2015) 9209–9213.

[28] H.S. Sun, M.F. Jackson, L.J. Martin, K. Jansen, L. Teves, H. Cui, S. Kiyonaka, Y. Mori, M. Jones, J.P. Forder, T.E. Golde, B.A. Orser, J.F. MacDonald, M. Tymianski, Suppression of hippocampal TRPM7 protein prevents delayed neuronal death in brain ischemia, Nat. Neurosci. 12 (2009) 1300–1307.

[29] Y. Liu, C. Chen, Y. Liu, W. Li, Z. Wang, Q. Sun, H. Zhou, X. Chen, Y. Yu, Y. Wang, N. Abumaria, TRPM7 is required for normal synapse density, learning, and memory at different developmental stages, Cell Rep. 23 (2018) 3480–3491.

[30] C. Jansen, J. Sahni, S. Suzuki, F.D. Horgen, R. Penner, A. Fleig, The coiled-coil domain of zebrafish TRPM7 regulates Mg·nucleotide sensitivity, Sci. Rep. 6 (2016) 33459.

[31] A. Fleig, V. Chubanov, TRPM7. Handb Exp Pharmacol 222 (2014) 521–546.

[32] Z.G. Zou, F.J. Rios, A.C. Montezano, R.M. Touyz, TRPM7, magnesium, and signaling, Int. J. Mol. Sci. 20 (2019) 1877.

[33] Y.L. Chun, M. Kim, Y.H. Kim, N. Kim, H. Yang, C. Park, Y. Huh, J. Jung, Carvacrol effectively protects demyelination by suppressing transient receptor potential melastatin 7 (TRPM7) in Schwann cells, Anat. Sci. Int. 95 (2020) 230–239.

[34] Y. Luo, J.Y. Wu, M.H. Lu, Z. Shi, N. Na, J.M. Di, Carvacrol alleviates prostate cancer cell proliferation, migration, and invasion through regulation of PI3K/Akt and MAPK signaling pathways, Oxid. Med. Cell. Longev. (2016), 1469693.

[35] T. Wang, S. Seah, X. Loh, C.W. Chan, M. Hartman, B.C. Goh, S.C. Lee, Simvastatin-induced breast cancer cell death and deactivation of PI3K/Akt and MAPK/ERK signalling are reversed by metabolic products of the mevalonate pathway, Oncotarget 7 (2016) 2532–2544.

[36] C. Hu, L. Huang, C. Gest, X. Xi, A. Janin, C. Soria, H. Li, H. Lu, Opposite regulation by PI3K/Akt and MAPK/ERK pathways of tissue factor expression, cell-associated procoagulant activity and invasiveness in MDA-MB-231 cells, J. Hematol. Oncol. 5 (2012) 16–25.

[37] E.R. Lee, J.Y. Kim, Y.J. Kang, J.Y. Ahn, J.H. Kim, B.W. Kim, H.Y. Choi, M.Y. Jeong, S.G. Cho, Interplay between PI3K/Akt and MAPK signaling pathways in DNA-damaging drug-induced apoptosis, BBA Mol, Cell. Res. 1763 (2006) 958–968.

[38] J.A. Fresno Vara, E. Casado, J. de Castro, P. Cejas, C. Belda-Iniesta, M. Gonzalez-Baron, PI3K/Akt signalling pathway and cancer, Cancer Treat, Rev 30 (2004) 193–204.

[39] S. Sathornsumetee, J.N. Rich, Designer therapies for glioblastoma multiforme, Ann. N. Y. Acad. Sci. 1142 (2008) 108–132.

[40] M. Yu, C. Huang, Y. Huang, X. Wu, X. Li, J. Li, Inhibition of TRPM7 channels prevents proliferation and differentiation of human lung fibroblasts, Inflamm. Res. 62 (2013) 961–970.

[41] L. Fang, S. Zhan, C. Huang, X. Cheng, X. Lv, H. Si, J. Li, TRPM7 channel regulates PDGF-BB-induced proliferation of hepatic stellate cells via PI3K and ERK pathways, Toxicol. Appl. Pharmacol. 272 (2013) 713–725.

[42] C. Garcia, L.G. Dubois, A.L. Xavier, L.H. Gerraldo, A.C.C. da Fonseca, A.H. Correia, F. Meirelles, G. Ventura, L. Romao, N.H.S. Canedo, J.M. de Souza, J.R.L. de Menezes, L. Romao, N.H.S. Canedo, J.M. de Souza, J.R.L. de Menezes, V. Moura-Neto, F. Tovar-Moll, F.R.S. Lima, The orthotopic xenotransplant of human glioblastoma successfully recapitulates glioblastoma microenvironment interactions in a non-immunosuppressed mouse model, BMC Cancer 14 (2014) 923.

[43] S. Suzuki, R. Penner, A. Fleig, TRPM7 contributes to progressive nephropathy, Sci. Rep. 10 (2020) 2333.

[44] E. Nishida, S. Maekawa, H. Sakai, Cofilin, a protein in porcine brain that binds to actin filaments and inhibits their interactions with myosin and tropomyosin, Biochemistry 23 (1984) 5307–5313.

[45] S. Nagai, O. Moreno, C.A. Smith, S. Ivanchuck, R. Romagnuolo, B. Golbourn, A. Weeks, H.J. Seol, J.T. Rutka, Role of the cofilin activity cycle in astrocytoma migration and invasion, Genes & Cancer 2 (2011) 859–869.
[46] H. Xiao, Effect of SSH1/SSH2 expression changes by shRNA in glioma cell lines on response to radiotherapy and cofilin-1 reactivation, Am. J. Clin. Oncol. 37 (2019), e13505.
[47] M.A. Oh, E.S. Kang, S.A. Lee, E.O. Lee, Y.B. Kim, S.H. Kim, J.W. Lee, PKCdelta and cofilin activation affects peripheral actin reorganization and cell-cell contact in cells expressing integrin alpha5 but not its tailless mutant, J. Cell. Sci. 120 (2007) 2717–2730.
[48] F. Deason-Towne, A.L. Perraud, C. Schmitz, Identification of Ser/Thr phosphorylation sites in the c2-domain of phospholipase c gamma2 (PLCγ2) using TRPM7-kinase, Cell Signal. 24 (2012) 2070–2075.
[49] C.Y. Jung, S.Y. Kim, C. Lee, Carvacrol targets AXL to inhibit cell proliferation and migration in non-small cell lung cancer cells, Anticancer Res. 38 (2018) 279–286.
[50] T. Saberbaghi, R. Wong, J.T. Rutka, G.L. Wang, Z.P. Feng, H.S. Sun, Role of Cl-channels in primary brain tumour, Cell Calcium. 81 (2019) 1–11.
[51] M. Faouzi, T. Kilch, F.D. Horgen, A. Fleig, R. Penner, The TRPM7 channel kinase regulates store-operated calcium entry, J Physiol. 595 (2017) 3165–3180.
[52] S. Chandra, D.J. Parker, R.F. Barth, S.C. Pannullo, Quantitative imaging of magnesium distribution at single-celled resolution in brain tumors and infiltrating tumor cells with secondary ion mass spectrometry (SIMS), J Neurooncol. 127 (2016) 33–41.